

FATIGUE CRACK GROWTH THRESHOLD CONDITIONS FOR SMALL NOTCHES

C. Vallellano, A. Navarro and J. Domínguez

Departamento de Ingeniería Mecánica y de los Materiales,
Escuela Superior de Ingenieros, Universidad de Sevilla,
Camino de los Descubrimientos s/n, 41092 Sevilla, SPAIN

ABSTRACT

The propagation or non-propagation of fatigue cracks from small notches is analysed in terms of a recently developed microstructural model which accounts for interactions between cracks and material barriers (such as, for example, grain boundaries) and which also incorporates the effect of the notch stress gradient. The term “small notches” refers here to stress concentration features whose size is of the same order as the characteristic microstructural size of the material. Typical examples of these small notches are pores, inclusions, pits and superficial scratches. Quantitative predictions for the fatigue limit are compared with experimental data reported in the literature for specimens of different materials containing small artificial defects.

INTRODUCTION

It is now well established that the fatigue strength of metallic materials is governed by the resistance to crack growth offered by microstructural barriers, e.g. grain boundaries, phase limits, precipitates, etc., present in the material. Experimental evidence shows that the conventional fatigue limit in plain specimens is not the critical stress under which cracks do not appear, but, rather, the threshold stress below which incipient cracks are unable to overcome the first few microstructural barriers and, thus, stop propagating [1,2]. Small material and manufacturing defects, such as pores, inclusions, pits and superficial scratches, are usually found in engineering components. The presence of these defects could help early cracks to overcome the first significant barriers and could, therefore, result in a reduction of the fatigue properties of the component. The effects of this type of defects may be analyzed by considering them as a particular case of notches the typical size of which is of the same order as the characteristic microstructural size of the material.

The experimental findings of a number of investigations on the significance of defects and small artificial notches (drilled holes) in the fatigue strength of materials might be summarized in four points. (1) Defects below a certain critical size do not affect the fatigue limit of the material (non-damaging notches) [3–6].(2) This critical size of defects shows a strong dependence on the static strength of the material. In the case of steels, for instance, sizes of non-damaging notches in high strength steels are

(3) For a particular material, the critical size seems to be generally smaller than the maximum non-propagating crack length observed at the fatigue limit in “defect-free” specimens [3–6]. (4) Cracks are always observed at the edges of the hole even at stresses well below the fatigue limit of the specimen; under stress levels less or equal the fatigue limit of the notched specimen, cracks propagate for a small distance and then arrest [3, 4].

The aim of the present paper is to show the ability of a recently developed model, based on Microstructural Fracture Mechanics concepts, to describe the fatigue behaviour of materials containing small notches or defects. The present model provides a micro-mechanical description of the fatigue crack propagation threshold conditions at notches which accounts for the interaction of the crack with material barriers (e.g. grain boundaries) and the effect of the stress gradient associated with the notch.

DESCRIPTION OF THE MODEL

Let us consider a crack growing from an elliptical notch in a semi-infinite body and interacting with the microstructure. Figure 1 depicts such a crack. The plastic zone of the crack is blocked at an internal microstructural barrier. From the small fatigue crack growth model for plain specimens developed by Navarro and de los Rios [8–10], the crack propagation process may be rationalized as follows. It is assumed that the crack tip plastic zone advances in jumps, that is, it is blocked at a barrier and remains blocked until the “pressure” that the crack exerts upon the barrier is high enough to activate plastic slip beyond the barrier. Once this happens, the plastic zone spreads to the next barrier, where it is blocked again and then the process is repeated. This is the way in which the crack is able to overcome the microstructural barriers.

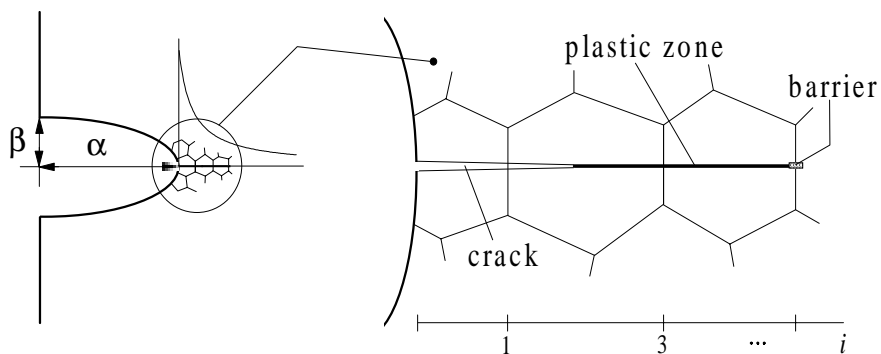


Figure 1: Schematic representation of the crack in a notched specimen.

The crucial factor differentiating the notched case from the plain one is that the pressure that the crack exercises upon the barrier can vary considerably from one barrier to the next due to the stress gradient associated with the notch. Thus, depending on the severity of this gradient and the level of applied stress, it might be possible for the crack to overcome the first few barriers, but, because of the decreasing stress field, it might be unable to overcome the following ones. If this were the case, the crack would become non-propagating. See [11, 13] for a more detailed description.

Using continuous distributions of infinitesimal dislocations and conformal mapping techniques, it is possible to find analytical solutions for a crack growing through the microstructure at the base of an elliptical notch in the simplest case of antiplane stress [11, 12]. In particular, it is possible to obtain a simple expression for the threshold stress τ_{Li}^N required for a crack to overcome a generic microstructural barrier in the material at a distance $iD/2$ from the notch root [11, 13], which is given by

$$\frac{\tau_{Li}^N}{\tau_{FL}} = \left(\frac{m_i^*}{m_1^*} \right) \frac{1}{\bar{\alpha} + \bar{\beta}} \left[\frac{\bar{\beta}}{\lambda_i} + \frac{\bar{\alpha}}{\sqrt{1 + \lambda_i^2}} \right]^{\frac{1}{2}} \quad i = 1, 3, 5, \dots \quad (1)$$

where $\lambda_i = \frac{1}{\bar{\alpha} + \bar{\beta}} \left[\bar{\alpha} \sqrt{(\bar{\alpha} + i)^2 - \bar{\alpha}^2 + \bar{\beta}^2} - \bar{\beta}(\bar{\alpha} + i) \right]$, $\bar{\alpha} = \alpha/(D/2)$ and $\bar{\beta} = \beta/(D/2)$ are the non-dimensional depth and width of the notch, and D is the characteristic microstructural size (e.g. the grain size or the mean free-path between barriers). τ_{FL} is the fatigue limit of the material, which may be interpreted as the minimum applied stress level below which cracks are unable to propagate beyond the first significant microstructural barrier. Finally, the term (m_i^*/m_1^*) represents the effective strength of the i -th barrier. This refers here to the resistance opposed by the material to plastic slip activation beyond a certain microstructural barrier. Thus, it is assumed that the term (m_i^*/m_1^*) stems mainly from two facts: the crystallographic opposition to plastic slip and the retardation mechanisms induced in the crack itself, *e.g.* crack closure. The crystallographic effect comes from the fact that, as the crack becomes longer, the crack front is forced to grow through a bigger number of grains not all favorably oriented. On the other hand, closure mechanisms reduce the pressure the cracks exerts upon the barriers and, so, its effect is simply represented in the model via enhanced values of the barrier resistance. Both effects lead to a progressive increase in the effective strength of successive barriers, until it reaches a saturated value for long cracks. As discussed in a previous paper [13], the evolution of the effective barrier strength may be determined from the well-known Kitagawa-Takahashi (K-T) diagram, the mathematical representation of which is given in micromechanical terms by the following equation

$$\frac{\tau_{Li}}{\tau_{FL}} = \left(\frac{m_i^*}{m_1^*} \right) \frac{1}{\sqrt{i}} \quad i = 1, 3, 5, \dots \quad (2)$$

where τ_{Li} represents the threshold stress to propagate a crack beyond the i -th barrier in a plain specimen. A practical expression for the evolution of (m_i^*/m_1^*) which renders the typical behaviour displayed by the K-T diagram in metallic materials has been also proposed in [13],

$$\frac{m_i^*}{m_1^*} = \frac{\sqrt{\bar{a}_0}}{\left(i^f + \bar{a}_0^f - 1 \right)^{\frac{1}{2f}}} \sqrt{i}, \quad (3)$$

where $\bar{a}_0 (= a_0/(D/2))$ is the dimensionless expression of the intrinsic crack length a_0 locating the typical knee of the Kitagawa-Takahashi diagram, and which is usually calculated as $a_0 = \frac{1}{\pi} (K_{th\infty}/Y\tau_{FL})^2$, $K_{th\infty}$ being the threshold stress intensity factor for long cracks and Y a crack-shape factor. The exponent f in Eq. 3 controls the speed at which the resistance of the barriers saturates. For metallic materials, values of f are generally bigger than unity [11, 13].

Equation 1 yields two threshold stresses of practical interest in notch fatigue. On the one hand, the fatigue crack initiation limit, which, in the micromechanical context presented here, may be interpreted as the minimum applied stress required to overcome the first microstructural barrier at the notch root. Thus, the initiation limit τ_{L1}^N is obtained simply making $i = 1$ in Eq. 1,

$$\tau_{L1}^N = \frac{\tau_{FL}}{\bar{\alpha} + \bar{\beta}} \left[\frac{\bar{\beta}}{\lambda_1} + \frac{\bar{\alpha}}{\sqrt{1 + \lambda_1^2}} \right]^{\frac{1}{2}} \quad (4)$$

On the other hand, the fatigue crack propagation limit τ_{FL}^N , corresponds with the minimum applied stress which ensures that the crack will be able to propagate across all microstructural barriers and,

simply satisfied by taking the maximum of the succession of threshold stresses given by Eq. 1,

$$\tau_{FL}^N = \max_i (\tau_{Li}^N) \quad i = 1, 3, 5, \dots \quad (5)$$

As can be seen in [13,14], in the case of notches of practical size, that is, $\bar{\alpha} \gg 1$, the present micromechanical model gives both qualitative and quantitative predictions highly consistent with experimental observations.

PREDICTED FATIGUE BEHAVIOUR FOR SMALL NOTCHES

The effect of small notches or defects can be studied using the equations given above for the particular case where $\bar{\alpha}$ is of the order of one or less than one. Two different sizes of elliptical defects are analysed in this section. The first case represents a defect of the same size than the characteristic microstructural length and we take $\bar{\alpha} = 1$. The second one corresponds to a defect substantially smaller than the microstructural size. We have taken a value of $\bar{\alpha} = 0.1$ in this case. To carry out the calculations reported bellow, the K-T diagram of the defect-free material has been approximated by Eqns. 2 and 3 using $\bar{a}_0 = 15$, according to Taylor's results [15], and $f = 2.5$ as a representative value for the saturation rate (see [13]).

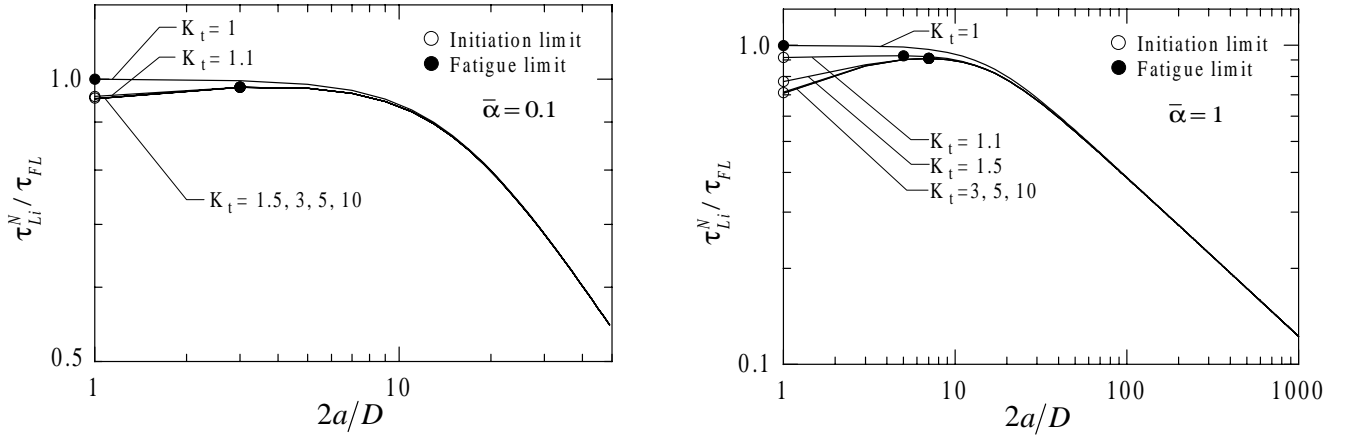


Figure 2: Threshold stress *vs.* crack length in specimens with small notches.

Figure 2 depicts the evolution of the threshold stresses given by Eq. 1 as a function of the crack length and different stress concentration factors ($K_t = 1.1, 1.5, 3, 5, 10$). Note that K_t equal to unity represents the defect-free material. It can be seen that the small-notch fatigue limit is only slightly smaller than fatigue limit of the defect-free material. Differences of only around 10% are found when the defect size is equal to the microstructural size. Thus, the results above correctly indicate that extremely small notches, such as superficial scratches or tiny spherical pores, produce no appreciable reduction in fatigue strength. This was noticed by Heywood [16] as early as 1962 in his classical book when discussing the incorrect estimates yielded in those cases by the pioneering theories of Neuber and Peterson on notch sensitivity and which could be of some importance for a correct understanding of surface finish effects in fatigue. This behaviour also agrees with more recent observations reported by Murakami *et al.* [3,4]. These authors carried out fatigue tests on specimens containing artificial small holes ranging in diameter from 40 to 200 μm . A variety of material were analysed. For 0.13% and 0.46% carbon steels, having an

10 μm and 55 μm respectively did not influence the fatigue limit. On the other hand, for 70-50 brass (grain size $\approx 45\mu\text{m}$) and Al 2017-T4 (grain size $\approx 89\mu\text{m}$ in the transverse direction), it was found that holes with 40 – 50 μm diameters did not reduce appreciably the fatigue limit. Non-propagating cracks were found even at the edges of the smallest defects in all these experiments. Similar observations have been also reported by Lukas *et al.* for small circumferential semi-circular notches in Copper and in a 2.25Cr-1Mo pressure vessel steel [5, 6].

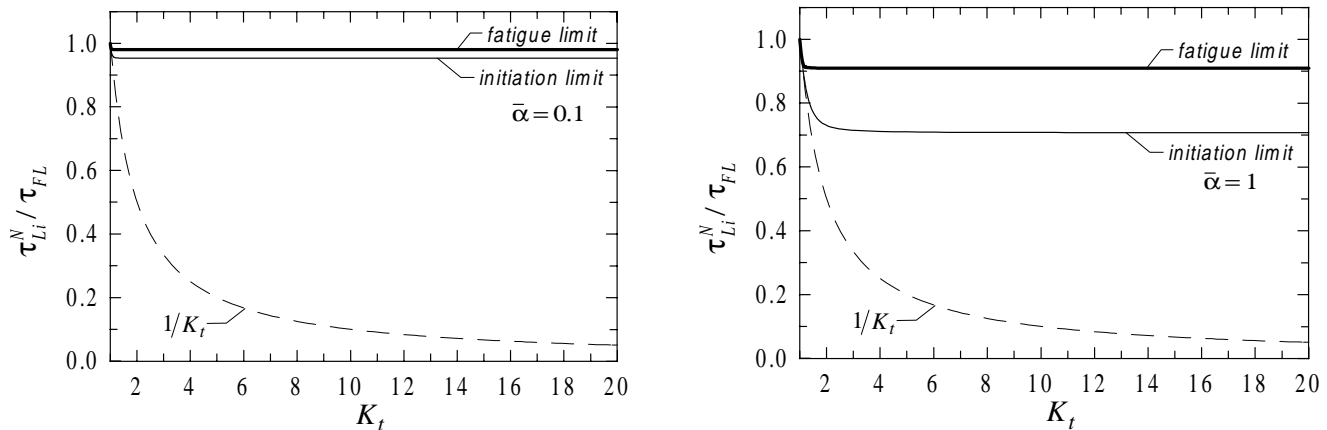


Figure 3: Initiation and propagation threshold stresses *vs.* K_t for small notches.

Figure 3 depicts again the results shown in Fig. 2 but in the format of the well-known Frost diagram. Here, it is possible to appreciate clearly the differences between the initiation and propagation threshold stresses. Two interesting trends may be observed. The first one is that, as the size of the notch decreases, the initiation and the fatigue limit approach and, as expected, both approach gradually the fatigue limit of the defect-free material. The second point is that both the initiation and the fatigue limits are fairly independent of the stress concentration factor. The influence of K_t is only appreciated at very low K_t values. The reason for this behaviour is that, even at stresses below the fatigue limit of the notched specimen, non-propagating cracks are well outside the effective notch stress zone [13]. The smaller the defect, the smaller the effective notch stress zone. This implies that it should be possible to study the fatigue effect of small notches without going too deep into the estimation of the exact K_t . For instance, they might be considered to be just small cracks.

This fact has indeed been pointed out by Murakami and colleagues in their works relating to the evaluation of the fatigue strength of materials containing defects with different shapes [7]. They found that small defects may be treated as small cracks and proposed relations for the notched fatigue limit in terms of $\sqrt{\text{area}}$ of the defect. The *area* parameter represents the area of the defect projected in direction of the maximum principal stress. The authors show a good agreement between experimental results and the predicted fatigue limit in a wide number of materials and type of defects, as long as there exist non-propagating cracks emanating from the defects.

An important effect which is intrinsically considered by the present model is the influence on the fatigue threshold conditions of the relative size of the notch as compared with the characteristic microstructural size of the material. Note that Eq. 1 depends on D via $\bar{\alpha}$ and $\bar{\beta}$. It follows, for instance, that a defect of a given size will be much more damaging in a fine-grained material (high $\bar{\alpha}$ value) than in a coarse-grained one (low $\bar{\alpha}$ value). This is consistent with the experimental observations, which show that low strength steels are able to sustain bigger defects than higher strength steels without any substantial

APPLICATION TO EXPERIMENTAL RESULTS

The equations obtained in the model were first developed for the simple case of elliptical notches under antiplane shear stresses. These equations were later generalized to cover the more practical case of notches of different shapes and subjected to axial tension. This generalization was based on the similarity shown by the stress distributions developed around notches of different geometry but which have the same value for the parameters K_t (stress concentration factor), α (notch size) and ρ (notch root radius). See [11, 14] for details. An expression for the threshold stresses in a notched specimen similar to Eq. 1 is obtained, but expressed now as a function of the three parameters mentioned above and the applied axial stress

$$\sigma_{Li}^N = \sigma_{Li} \frac{\sqrt{iD/2}}{K_t} \left[\frac{1}{\lambda_i \sqrt{\alpha \rho}} + \frac{(K_t - 1)^2}{\alpha \sqrt{1 + \lambda_i^2}} \right]^{\frac{1}{2}} \quad (6)$$

where $\lambda_i = \frac{\sqrt{\alpha \rho}}{\alpha - \rho} [\sqrt{1 + (iD/2)/\rho(2 + (iD/2)/\alpha)} - (1 + (iD/2)/\alpha)]$.

All the expressions used in the model and presented so far are based on solutions for the semi-infinite body problem. Therefore, the range of practical application of these expressions should be limited to small notch size / specimen's net width ratios. Ratios up to 0.2 provide reasonably accurate results as shown in [11].

Fatigue tests performed by Lukas *et al.* [5, 6] for specimens containing small notches have been analysed using the present model. The materials studied were electrolytic copper (99.98%Cu, fatigue limit $\sigma_{FL} = 73 \text{ MPa}$, $K_{th\infty} = 2.5 \text{ MPa}\sqrt{m}$) and a pressure vessel steel (2.25Cr/1Mo, $\sigma_{FL} = 220 \text{ MPa}$, $K_{th\infty} = 6 \text{ MPa}\sqrt{m}$). The grain size for copper specimens was $50\mu m$. For the steel specimens the mean packet size of bainite was $30\mu m$. Cylindrical specimens of 5 mm diameter with circumferential semicircular notches of radii ranging from 10 to $800\mu m$ were tested under symmetrical loading conditions ($R = -1$). Notched specimen data and experimental fatigue limits (amplitudes) are shown in Table 1.

TABLE 1
EXPERIMENTAL AND PREDICTED NOTCHED FATIGUE LIMIT ($R = -1$).

| Material | $\alpha = \rho$ (mm) | K_t | σ_{FL}^N (Exp.) (MPa) | σ_{FL}^N (Pred.) (MPa) |
|---------------------|-------------------------|-------|---------------------------------|----------------------------------|
| steel 2.25Cr/1Mo | 0.01 | 3.04 | 216.5 - 228.5 | 216.3 |
| | 0.03 | 2.99 | 214 - 228 | 199 |
| | 0.05 | 2.95 | 196 - 226 | 187.5 |
| | 0.07 | 2.92 | 160 - 170 | 176.5 |
| | 0.20 | 2.67 | 135.5 - 145.5 | 141.2 |
| | 0.41 | 2.32 | 145 - 155 | 120.8 |
| Copper | 0.05 | 2.95 | 70 - 74 | 62 |
| | 0.10 | 2.87 | 54 - 58 | 55.8 |
| | 0.15 | 2.76 | 45.3 - 49.3 | 51.6 |
| | 0.20 | 2.67 | 47 - 51 | 48.5 |
| | 0.30 | 2.51 | 45 - 49 | 44.2 |

The authors also determined K-T diagrams for plain specimens in both materials. The experimental results are shown in Fig. (a). The steel used for this purpose was nominally the same as the steel used in

Figure (a) also shows the fitting of Eqs. 2 and 3, expressed now in term of axial stresses. The values of exponent f are 2.5 and 1.65 for steel and copper respectively. The estimated crack-shape factor is about 0.8 in both cases. This is not very different from the theoretical figure of 0.65 that would be obtained in the case of perfectly semicircular cracks. As a matter of fact, the authors found nearly semi-circular cracks in those tests [6]. The pattern in notched specimens was slightly different. Cracks appeared to be of a somewhat distorted semi-circular shape when observed in short portions, but when longer portions were examined, they revealed an almost uniform depth [6]. It is expected, therefore, that cracks in notched specimens exhibit an average shape factor a bit higher than in plain specimens. A shape factor of unity has been assumed in the calculations reported here.

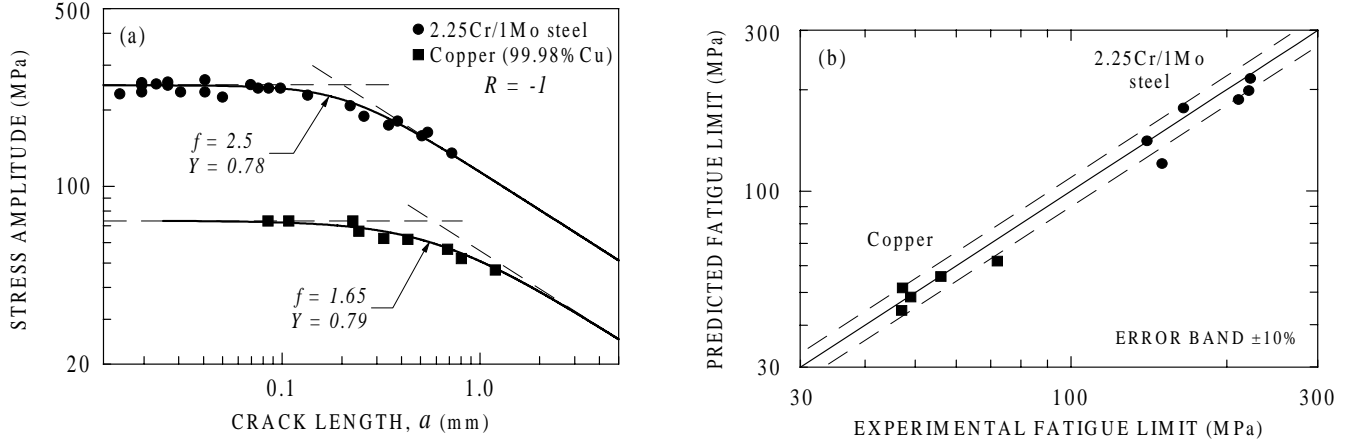


Figure 4: (a) Kitagawa-Takahashi diagram for 2.25Cr-1Mo steel and Copper. (b) Experimental and predicted notched fatigue limit.

The fatigue limits predicted using Equation 6 for copper and steel notched specimens are also shown in Table 1. As it can be seen, the predicted values are in reasonable agreement with their experimental counterparts. Figure (b) depicts graphically the differences between experiments and predictions. Here, the experimental fatigue limit corresponds with the mean value of the experimental range. It can be seen that differences are within, or very close to, an error band about 10% for both steel and copper specimens.

CONCLUSIONS

The micromechanical description of the fatigue crack growth threshold conditions at notches developed in the present model, based on the crack interaction with microstructural barriers and the notch stress gradient effect, provides an appropriated framework to analyse the fatigue behaviour of small notches or defects in metallic engineering components.

The evolution of the fatigue crack initiation limit and the conventional notch fatigue limit as a function of the defect size has been obtained. Qualitative predictions agree well with the experimental evidence reported in the literature. In particular, it has been shown that (1) For applied stresses bellow the fatigue limit of the specimen, cracks are generated at small notches or defects at a very early stage and they may be able to overcome just a few microstructural barriers before arresting at one of these barriers and becoming non-propagating. (2) If the size of the defect is smaller than the characteristic microstructural size of the material, the fatigue limit is not substantially altered. As expected, the finer the microstructure (higher ultimate tensile strength) the smaller the size of non-damaging notches. And (3), the initiation limit and the conventional fatigue limit of a specimen with a small notch are fairly

only at very low R_t values.

Finally, fatigue test performed by Lukas *et al.* for specimens of copper and 2.25Cr-1Mo pressure vessel steel containing small notches has been analysed using the present model. Quantitative predictions of the model are in good agreement with the experimental results.

ACKNOWLEDGEMENTS The authors thank the Spanish Ministry of Education for its financial support through grant PB97-0696-C02-01 and the Beca de Formación de Profesorado Universitario for C. Vallellano.

REFERENCES

1. Miller, K.J. (1993). *Material Science and Technology* **9**, 453.
2. Miller, K.J. (1997). In: *Fatigue and Fracture Mechanics*, pp. 267-286, Piascik, R.S., Newman, J.C. and Dowling, N.E. (Eds). ASTM STP **1296**.
3. Murakami, Y. and Endo, T. (1980). *Int. J. Fatigue* **2**, 23.
4. Murakami, Y., Tazunoki, Y. and Endo, T. (1984). *Met. Trans. A* **15A**, 2029.
5. Lukas, P., Kunz, L., Weiss, B. and Stickler, R. (1986). *Fatigue Fract. Engng. Mater. Struct.* **9**, 195.
6. Lukas, P., Kunz, L., Weiss, B. and Stickler, R. (1989). *Fatigue Fract. Engng. Mater. Struct.* **12**, 175.
7. Murakami, Y. and Endo, M. (1983). *Engng. Fract. Mech.* **17**, 1.
8. Navarro, A. and de los Rios, E.R. (1988). *Phil. Mag.* **57**, 15.
9. de los Rios, E.R. and Navarro, A. (1990). *Phil. Mag.* **61**, 435.
10. Navarro, A. and de los Rios, E.R. (1992). *Proc. R. Soc. Lond. A* **437**, 375.
11. Vallellano, C. (1999). PhD. Thesis, University de Sevilla, Spain.
12. Navarro, A., Vallellano, C., de los Rios, E.R. and Xin, X.J. (1999). In: *Engineering Against Fatigue*, pp. 63-72, Beynon, J.H., Brown, M.W., Smith, R.A., Lindley, T.C. and Tomkins, B. (Eds). A.A. Balkema, Rotterdam.
13. Vallellano, C., Navarro, A. and Dominguez, J. (2000). *Fatigue Fract. Engng. Mater. Struct.* **23**, 113.
14. Vallellano, C., Navarro, A. and Dominguez, J. (2000). *Fatigue Fract. Engng. Mater. Struct.* **23**, 123.
15. Taylor, D. (1982). *Fatigue Engng. Mater. Struct.*, **5**, 305.
16. Heywood, R.B. (1962). *Designing against Fatigue*. Chapman & Hall, London.